Mon. Not. R. astr. Soc. (1966) **132**, 463–470.

THE RELATIVE ABUNDANCE OF SILICON, IRON AND NICKEL IN THE SOLAR CORONA

Carole Jordan

(Communicated by the Director, University of London Observatory)

(Received 1965 July 21)

Summary

The method of analysis, developed by Pottasch, for determining the relative abundance of elements represented in the far ultra-violet part of the solar spectrum has been extended to include recently identified lines of iron and nickel. The calculations of the ionization equilibrium included the process of dielectronic recombination. The results indicate that the abundance of iron relative to nickel is the same in the corona as in the photosphere, but that the abundance of iron relative to silicon is an order of magnitude larger in the corona than in the photosphere. The distribution of

$$\int_R N_e^2 dh$$

with temperature now indicates a general coronal temperature of $1{\cdot}4 \times 10^6$ °K and a decrease in the quantity of coronal material for temperatures in excess of this value.

1. *Introduction.* In recent papers, Pottasch (**1, 2**), has developed a method of determining the abundance of elements in the solar chromosphere and corona, from the intensities of emission lines in the far ultra-violet part of the solar spectrum. His results included a value of the relative abundance of silicon and iron, but at the time of his investigation only the lines of Fe XV and Fe XVI were definitely identified.

The present work is an extension of his method using the recently classified lines of iron and nickel, most of which are observed in the solar spectrum (**3, 4**). The abundances of iron and nickel have been found relative to silicon. The distribution of

$$\int_R N_e^2 \, dh,$$

where N_e is the electron density, with temperature, for temperatures greater than 10^6 °K has been improved, and for the first time shows the decrease in the amount of coronal material at very high temperatures. Also, the ionization equilibrium has been calculated taking into account the effect of di-electronic recombination.

2. *Method of analysis.* The method of analysis developed by Pottasch is as follows. The intensity of a solar emission line can be expressed as:

$$E = 2{\cdot}4 \times 10^{-20} f_{ij} \frac{N(E)}{N(H)} P\left(\frac{W_{ij}}{kT_e}\right) \int 10^{-5040 W_{ij}/T_e} \frac{N(\text{ion})}{N(E)} T_e^{-1/2} N_e^2 \, dh \qquad (1)$$

where E is the intensity at the Earth's distance in erg cm^{-2} s^{-1}; $N(E)$ and $N(H)$ are the abundance of a given element and of hydrogen, respectively; N(ion) is the number density of a given ion; T_e is the electron temperature; f_{ij} is the oscillator strength; W_{ij} is the excitation energy in electron volts, and $P(W_{ij}/kT_e)$ is an integral of the Gaunt factor. For a given stage of ionization, the function under the integral in equation (1), can be expressed as

$$g(T) = T_e^{-1/2}\, 10^{-5040 W_{ij}/T_e} \frac{N(\text{ion})}{N(E)}. \qquad (2)$$

This function has a fairly sharp maximum at a certain temperature, $T_{\max}$, and it can be assumed that an observed spectrum line is formed in the region where the temperature is close to $T_{\max}$. The integral over height in equation (1) can then be limited to the region R, where the temperature is close to $T_{\max}$. Within this region it can be assumed that

$$g(T) = 0{\cdot}7\, g(T)_{\max}.$$

Then, if for a given line, the intensity, oscillator strength and excitation energy are known, the quantity

$$\frac{N(E)}{N(H)} \int_R N_e^2\, dh$$

can be calculated. If several stages of ionization are represented,

$$\frac{N(E)}{N(H)} \int_R N_e^2\, dh$$

may be plotted against $T_{\max}$. The relative abundance of various elements may be found by fitting the curve for each to that of a chosen element.

3. *The calculations for silicon, iron and nickel*

(*a*) *The effect of including dielectronic recombination.* A general formula provided by Burgess (**5**) has been used to calculate the rate of di-electronic recombination for the ions of interest, and the total recombination rate, di-electronic + radiative, has been used in the present evaluations of the ionization equilibrium. The effect of the increased recombination rate is to increase the temperature at which a given ion has maximum abundance and to increase the temperature range over which $g(T) = 0{\cdot}7\, g(T)_{\max}$ (**6**). The final value of

$$\frac{N(E)}{N(H)} \int_R N_e^2\, dh$$

for each ion is hardly altered. The ionization rate and radiative recombination rate used are those of Burgess & Seaton (**6**). The collisional excitation rate is taken from Van Regemorter (**7**).

(*b*) *Data used in the present calculations.* The intensity data are from the spectrum of Hall *et al.* (**8**), taken in 1964 March. These intensities are similar to those from their earlier spectrum, taken in 1963 May (**9**), except that the intensity of the Fe XV line at 284 Å was less in 1964 March.

The f values for the transitions of the type $2s^2 2p^n - 2s2p^{n+1}$ in silicon and $3s^2 3p^n - 3s3p^{n+1}$ in iron and nickel have been taken from the work of Varsavsky (**10**), except for Si x, Fe x and Fe xiv where Garstang's (**11**) values have been. Other f values have been calculated by the present author using the method of Bates & Damgaard (**12**).

Table I gives the lines, intensities and f values used in the present analysis. For the silicon lines, the f values from Bates–Damgaard calculations are given as a comparison with Varsavsky's values. Table I also includes the calculated values of log $T_{\max}$,

$$\log \frac{N(\text{ion})}{N(E)}, \text{ and } \log \frac{N(E)}{N(H)} \int_R N_e^2 \, dh.$$

The tabulated value of the latter is generally a mean for the listed lines of an ion. Only lines which are formed predominantly by collisional excitation from the ground level, followed by emission, are included in the table. Other lines will be weakened by the underpopulation of the excited levels of the ground term, and if their intensities are used in equation (1), they will give values of

$$\frac{N(E)}{N(H)} \int_R N_e^2 \, dh$$

which are too small (**3, 13**).

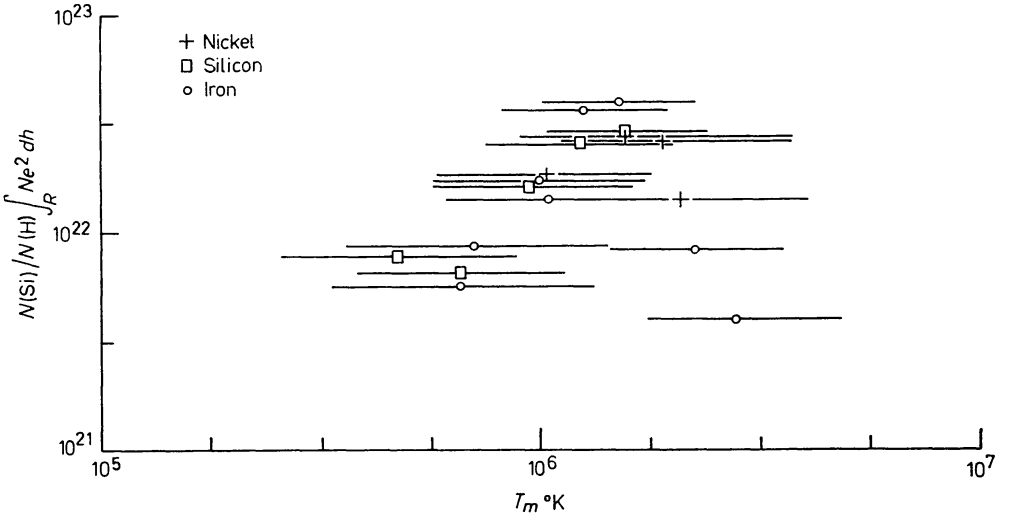

FIG. 1. $\frac{N(Si)}{N(H)} \int_R N_e^2 \, dh$ *plotted against* $T_{\max}$, *the curves for Fe and Ni having been fitted to that of Si to give the relative abundance.*

4. *Discussion of results*

(*a*) *Relative abundances.* For silicon, iron and nickel a graph of

$$\frac{N(E)}{N(H)} \int_R N_e^2 \, dh$$

was plotted against log $T_{\max}$. The abundances of iron and nickel relative to silicon, were found by fitting their curves to that of silicon, and Fig. 1 shows the final graph. The horizontal lines indicate the temperature range of the integral for each ion. The results are given in Table II, together with the values of the

TABLE I

Data used in the present analysis, and the results

Ion	Transition	ΔJ	λ (Å)	f_{ij} V	f_{ij} B–D	log E (erg cm^{-2} s^{-1})	log T_{max} (°K)	log $\frac{N(ion)}{N(E)}$	log $\frac{N(E)}{N(H)}\int_R N_e^2\, dh$
Si VI	$2s^22p^5\ ^2P$	3/2–1/2	246·0	0·16	0·08	−2·72	5·68	−0·24	21·89
	$-2s2p^6\ ^2S$	1/2–1/2	249·4	0·16	0·08	−3·00			
Si VII	$2s^22p^4\ ^3P$	2–2	275·4	0·25	0·15	−2·89	5·82	−0·33	21·82
	$-2s2p^5\ ^3P$	1–1							
		1–2	278·4	0·11	0·07	−2·80			
		2–1	272·6b	0·06	0·04	−3·15			
Si VIII	$2s^22p^3\ ^2D$	5/2–5/2	277·1	0·26	0·16	−2·44	5·98	−0·32	22·22
	$-2s2p^4\ ^2D$	3/2–3/2	276·8						
	$-2s2p^4\ ^2P$	5/2–3/2	216·9	0·14	0·09	−2·46			
		3/2–1/2	214·8	0·12	0·07	−2·92			
Si IX	$2s^22p^2\ ^3P$	2–1, 2	296·2	0·07	0·05	−2·49	6·09	−0·42	22·41
	$-2s2p^3\ ^3P$	1–0, 1, 2	292·8	0·07	0·05	−2·70			
		0–1	290·5b	0·07	0·05	−2·77			
	$-2s2p^3\ ^3S$	0–1	227·0b	0·10	0·07	−2·34			
		1–1	225·0b	0·10	0·07	−2·28			
				G					
Si X	$2s^22p\ ^2P$	3/2–1/2	261·2b	0·045		−2·66	6·20	−0·36	22·46
	$-2s2p^2\ ^2P$	1/2–1/2	256·6	0·12		−2·09			
	$-2s2p^2\ ^2S$	1/2–1/2	272·0	0·043		−2·66			
				B–D					
Fe VIII	$3p^63d\ ^2D$	3/2–5/2	130·9	0·24		−2·74	5·86	−0·16	22·02
	$-3p^64f\ ^2F$	5/2–7/2	131·2	0·25					
	$-3p^53d^2\ ^2D$	3/2–3/2	167·5	0·5?		−2·55	5·82	−0·13	21·84
		3/2–5/2	167·7						
		5/2–3/2	168·0						
		5/2–5/2	168·2	0·5?		−2·46			
	$-3p^53d^2\ ^2F$	5/2–7/2	185·2	0·5?		−2·21	5·80	−0·12	

TABLE I (*continued*)

Ion	Transition	ΔJ	λ (Å)	f_{ij}	log E (erg cm^{-2} s^{-1})	log T_{max} (°K)	log $\frac{N(\text{ion})}{N(E)}$	log $\frac{N(E)}{N(H)}\int_R N_e^2\, dh$
				B–D				
Fe IX	$3p^6\ ^1S$	0–1	171·1	3·34	−1·34	6·00	−0·43	22·33
	$-3p^5 3d\ ^1P$							
	$-3p^5 4s\ ^1P$	0–1	103·6	0·2?	−2·85	6·02	−0·43	22·25
Fe X	$3p^5\ ^2P$	3/2–5/2	174·5	1·51	−1·35	6·10	−0·49	22·67
	$-3p^4 3d\ ^2D$							
	$-3p^4 3d\ ^2P$	3/2–3/2	177·2	0·66	−1·43			
Fe XI	$3p^4\ ^3P$	2–3	180·4	1·08	−1·32	6·18	−0·54	22·70
	$-3p^3 3d\ ^3D$							
				G				
Fe XIV	$3p\ ^2P–3d\ ^2D$	1/2–3/2	211·3	0·55	−2·21	6·36	−0·56	22·03
	$3s^2 3p\ ^2P$	1/2–1/2	274·2	0·215	−2·47			
	$-3s3p^2\ ^2S$							
				V				
Fe XV	$3s^2\ ^1S$	0–1	284·2	1·18	−2·15	6·44	−0·63	21·70
	$-3s3p\ ^1P$							
				B–D				
Ni X	$3p^6 3d\ ^2D -$	3/2–3/2	144·2	0·44?	−3·00?	6·02	−0·10	21·26
	$3p^5 3d\ ^2D$	5/2–5/2	145·0	0·44?	−2·84			
	$3p^5 3d^2\ ^2F$	5/2–7/2	158·4	0·44?	−2·84			
		3/2–5/2	160·0	0·44?	−2·84			
Ni XI	$3p^6\ ^1S$	0–1	148·4	2·95	−2·17	6·20	−0·50	21·44
	$-3p^5 3d\ ^1P$							
Ni XII	$3p^5\ ^2P$							
	$-3p^4 3d\ ^2D$	3/2–5/2	152·1	1·30	−2·48	6·28	−0·41	21·42
	$-3p^4 3d\ ^2P$	3/2–3/2	154·2	0·57	−2·72			
Ni XIII	$3p^4\ ^3P$							
	$-3p^3 3d\ ^3D$	2–3	157·8	0·95	−2·84	6·32	−0·45	21·14

TABLE II

The abundance of silicon, iron and nickel

	Photosphere		Corona		
(i) Relative values	Goldberg *et al.* (**14**)	Aller *et al.* (**15**)	Warner (**16**)	Pottasch (**17**) (from forbidden lines)	Jordan (from permitted XUV lines)
$\log \frac{N(\mathrm{Si})}{N(\mathrm{Fe})}$	+1·00	+1·00	+0·88	—	−0·10
$\log \frac{N(\mathrm{Fe})}{N(\mathrm{Ni})}$	+0·90	—	+1·20	+1·15	+1·10
(ii) Values on the scale $\log N(\mathrm{H}) = 12{\cdot}00$					
$\log N(\mathrm{Si})$	7·50	7·50	7·69	—	(7·70)
$\log N(\mathrm{Fe})$	6·51	6·59	6·81	7·87	(7·80)
$\log N(\mathrm{Ni})$	5·62	—	5·61	6·72	(6·70)

abundance of silicon, iron and nickel as found from photospheric analyses (**14–16**), and from the coronal forbidden lines (**17**). The results have been expressed as relative abundances, and it can be seen that: (i) the abundance of iron relative to nickel is the same in the corona as in the photosphere, and (ii) the abundance of iron relative to silicon is an order of magnitude larger in the corona than in the photosphere.

Radio observations of the corona at times near sunspot minimum indicate maximum temperatures of only 8×10^5 °K, as against the temperature of about $1{\cdot}5 \times 10^6$ °K found from the ultra-violet data. For this reason the author considers that a reliable value of the absolute abundance of, for example, silicon, cannot be found by comparing the ultra-violet data used in the present analysis, with radio data, as performed by Pottasch (**1, 2**). However, although no absolute abundance has been found, the results can be compared with other determinations in the following way. All methods of analysis of the coronal lines of iron, whether permitted or forbidden lines, lead to an abundance of iron of about 7·80, on the scale of $\log(H) = 12{\cdot}00$. Fitting the relative abundances to this value gives an abundance of silicon of 7·70, slightly larger than the photospheric value of 7·56, and an abundance of nickel of 6·70.

(*b*) *Sources of error.* The relative values of the oscillator strengths used for iron and nickel should be reliable, as these elements are almost adjacent in atomic number. The disagreement of a factor of 10 between the photospheric and coronal values of

$$\log \frac{N(\mathrm{Fe})}{N(\mathrm{Si})},$$

is unlikely to be explained on the basis of errors in f values. The f sum rule states that $\sum f$ from a given level, in this case the ground level, should equal the number of equivalent electrons in the configuration from which the excitation takes place. Checking the f values of the iron and nickel lines given in Table I, against this rule, shows that it is unlikely that the values are too small. If they are too large, the disagreement in relative abundance is increased. Considering the f values for silicon; Varsavsky estimates that his f values are reliable to an accuracy of not greater than 10%. A comparison of his values with those from Bates–Damgaard calculations shows agreement within a factor of 2.

It is possible that the intensity data used are in error below 256 Å, as the spectrum taken in 1964 March, was calibrated only at 304 Å and 256 Å. The silicon lines lie at wavelengths between 220 and 296 Å, so their intensities should be reasonably correct. The iron lines lie mainly between 165 and 220 Å, so that an unsuspected change in sensitivity with wavelength could introduce an error in the final relative abundance of silicon and iron. The nickel lines lie between 144 and 160 Å. The agreement of the relative abundance of nickel and iron found by the present method, with values from other methods, suggests that between 144 and 220 Å, errors due to uncertainties in calibration are small.

(*c*) *The variation of* $\int_R N_e^2\,dh$ *with* $T_{\max}$. The further iron and nickel data have enabled the distribution of

$$\int_R N_e^2\,dh$$

with temperature to be improved for temperatures greater than 10^6 °K. The maximum of the distribution occurs at $1{\cdot}4 \times 10^6$ °K, indicating that this is the general temperature of the corona. The work of Neupert (**18**), using results from O.S.O. – 1, has shown that lines of Fe XIV, XV and XVI undergo a temporal variation correlated with solar activity. If the variation is associated with local increases in the density and temperature of the corona, it would be expected that the part of the graph for temperatures above 2×10^6 °K would reflect such variations. If the observations of Hinteregger (**19**) in 1961 are used, the points for Fe XIV–XVI lie considerably above those shown in Fig. 1. The observations in 1964 March, at a time near sunspot minimum, show that only a small part of the coronal material is normally at temperatures greater than 2×10^6 °K.

Acknowledgments. The author wishes to thank Professor C. W. Allen for his advice, and Mr K. Phillips for his assistance with computations. The author acknowledges the support of a grant from the Science Research Council.

University of London Observatory,
London, N.W.7:

1965 *July.*

References

(1) Pottasch, S. R., 1963. *Astrophys. J.*, **137**, 945.
(2) Pottasch, S. R., 1964. *Space Sci. Rev.*, III, 5/6, 816.
(3) Gabriel, A. H., Fawcett, B. C. & Jordan, C., 1965. *Nature, Lond.*, **206**, 390.
(4) Gabriel, A. H. & Fawcett, B. C., 1965. *Nature, Lond.*, **206**, 808.
(5) Burgess, A., 1965. *Astrophys. J.*, **141**, 1588.
(6) Burgess, A. & Seaton, M. J., 1964. *Mon. Not. R. astr. Soc.*, **127**, 355.
(7) Van Regemorter, H., 1962. *Astrophys. J.*, **136**, 906.
(8) Hall, L. A., Schweizer, W., Heroux, L. & Hinteregger, H. E., 1965. *Astrophys. J.*, **142**, 13.
(9) Hinteregger, H. E., Hall, L. A. & Schweizer, W., 1964. *Astrophys. J.*, **140**, 319.
(10) Varsavsky, C., 1961. *Astrophys. J. Suppl. Ser.*, **6**, 75.
(11) Garstang, R. H., 1962. *Annls Astrophys.*, **25**, 109.
(12) Bates, D. R. & Damgaard, A., 1949. *Phil. Trans. R. Soc.*, A, **242**, 101.
(13) Jordan, C., 1965. *Mon. Not. R. astr. Soc.*, **132**, 515.
(14) Goldberg, L., Muller, E. A. & Aller, L. H., 1960. *Astrophys. J. Suppl. Ser.*, **5**, 1.
(15) Aller, L. H., O'Mara, B. J. & Little, S. J., 1964. *Proc. natn. Acad. Sci.*, **51**, 1238.
(16) Warner, B., 1964. Thesis, University of London.
(17) Pottasch, S. R., 1964. *Mon. Not. R. astr. Soc.*, **128**, 73.
(18) Neupert, W. M., 1965. *Annls Astrophys.*, **28**, 446.
(19) Hall, L. A., Damon, K. R. & Hinteregger, H. E., 1964. *Space Research*, Volume 3, p. 743 (Ed. Priester). North-Holland, Amsterdam.